Journal of Materials Chemistry B

Accepted Manuscript

ROYAL SOCIETY OF CHEMISTRY

www.rsc.org/materialsB

Functionalized carbon dots enable simultaneous bone crack detection and drug deposition

A. Shanti Krishna[a], C. Radhakumary[a*], Molly Antony[b], and K. Sreenivasan[a,*]

[a] Laboratory for Polymer Analysis, Biomedical Technology Wing, Sree Chitra Tirunal Institute for Medical Sciences & Technology, Thiruvananthapuram-695012, India.

[b] Department of Microbiology, Sree Chitra Tirunal Institute for Medical Sciences & Technology, Thiruvananthapuram-695011, India.

**Phone 091- 471 -2520248, Fax. 091- 471- 2341814. Email: sreeni@sctimst.ac.in, radha.changerath@gmail.com*

ABSTRACT

Recently, Carbon dots (CDs) have become one of the most sought nanomaterials for biological applications owing to their excellent fluorescence, chemical inertness and biocompatibility. This manuscript depicts the generation of a fluorescent nano probe using CDs for viewing bone cracks and simultaneous drug delivery to the cracked or infected sites. Water soluble polyethylene glycol diamine capped CDs were conjugated with glutamic acid (GA), a calcium targeting ligand, and ciprofloxacin as an antibacterial model drug. Physicochemical characterizations, cytotoxicity evaluation, haemolysis and antibacterial activity studies of the synthesized probe and its ability to target onto bone are demonstrated. Our results indicate that there is significant scope in negotiating functionalized CDs as theranostic agents.

Key words: Carbon dots, nano probes, fluorescence, drug delivery, bone cracks.

Introduction

Fluorescent nanoprobes are of great importance in biomedical research. A variety of nanomaterials such as quantum dots, metal nanoclusters, nanocrystals, silica- dye hybrid nanoparticles etc have been widely investigated for various applications[1-4]. Among a wide variety

of nanosized materials, semiconductor quantum dots is a forerunner for bioimaging applications. The toxicity and water insolubility of semi conductor quantum dots, however, limit their application in biomedical fields. Recently, nanosized CDs have been studied as benign probes in drug delivery and imaging applications owing to their acceptable fluorescence and biocompatibility[5-7]. CDs have several advantages, such as chemical inertness, lack of blinking, size and excitation-wavelength (λex) dependent photoluminescence, and amphiphilic characteristics depending on the surface capping materials[8-11]. These features along with non toxicity and biocompatibility make CDs ideal candidates for investigating biological systems[12].

Bone diseases comprise a variety of skeletal-related disorders such as arthritis, osteoporosis, osteoarthritis, osteosarcoma, and metastatic bone cancer resulting in major mobility hindrance and mortality to human beings[13]. Osteoporosis vary in degree of degeneration at different skeletal sites, unfortunately even with proven therapies, fractures at vital points like hip, spine etc are common, giving pain, discomfort and even depression to the older people[14]. In this context, multifunctional 'smart' entities with the ability to sense, diagnose, image and cure numerous ailments have tremendous possibilities[15]. The use of tools of nanotechnology in drug delivery for treating various orthopedic diseases is important when considering bone regeneration using bone implants and replacement strategies[16].

In many occasions, hairline cracks which are undetected initially later become site for infection leading to further misery. New strategies to address these issues are currently focused on designing nanoparticles capable of docking onto crack. To achieve specificity, nanoparticles are functionalized with bone targeting molecules. By this approach, simultaneous crack visualization and site specific drug delivery could be achieved.

New targeting strategies are employed to deliver drugs to the bone cracks which include fusion proteins or nanoparticles with targeting functionalities[17]. Bone cracks release calcium[18] which could be detected by incorporating molecules having calcium affinity within the drug delivery vehicle. Calcium content in the adult human body is approximately 1kg, and bone contains 99% of the total body calcium[19]. Glutamic acid (GA), a naturally occurring amino acid, well known for its calcium affinity has been used for targeted labeling of calcium rich sites like bone cracks and calcified tissues. It is reported that gold nanoparticles functionalized with GA has been used for targeting damaged bone tissue[20]. GA and aspartic acid peptides were reported being used for both bone-targeting and drug delivery purposes[21].

Ciprofloxacin, a fluoroquinolone drug was chosen in this study as a model drug owing to its antibacterial activity. It is the most commonly used antibiotic to treat infections of urinary tract, abdomen, bone and skin. Fluoroquinolones are valued for their broad spectrum of activity, excellent tissue penetration, and their availability in both oral and intravenous formulations[22].

In healthy individuals, bone resorption and formation are well balanced with the bone mass maintained in a steady state. Disturbances of this balance are characteristic of a number of bone diseases including osteoporosis, Paget's disease and bone cancer[23]. The advantages of a bone-targeted drug delivery system for the treatment of bone diseases are obvious. Such a system could easily impart osteotropicity to a variety of bone drugs and improve their therapeutic potential[24]. CD modified with calcium targeting ligands seems to have potential to locate bone cracks through fluorescence imaging. It is recently reported that CD based probes containing GA may be used to map calcium rich sites as well as bone cracks[25].

Here, amino functionalized CDs prepared as reported earlier[26] were conjugated with GA and ciprofloxacin simultaneously via EDC chemistry to locate bone cracks and deliver

appropriate drugs to facilitate rapid healing and check infection. This communication details the formation of functionalized probe, its physico-chemical characterizations, cytotoxicity evaluation, and preliminiary blood compatibility by haemolysis study, assessment of antibacterial activity and also demonstrates its ability to target bone cracks using freshly collected bone from slaughter house and cracks made manually.

Experimental

Materials

Citric acid anhydrate, PEG diamine, L-glutamic acid (GA), Ciprofloxacin, N-(3-Dimethylaminopropyl)-N'ethylcarbodiimide (EDC) and ninhydrin were obtained from Sigma Aldrich, Bangalore, India. All other chemicals used were of analytical grade and obtained from Merck India Ltd, Mumbai, India.

Synthesis of Carbon Dots (CD)

Amino functionalized carbon dots were synthesized as reported by Wang et al[26]. Briefly, 9 mL of glycerin and 600 mg of PEG diamine were taken in a 100 mL three-neck flask degassed with nitrogen. When the temperature was raised to 250°C, 600 mg of citric acid was added and allowed to react at this temperature for 3 h. The resulting product was cooled to room temperature and dialyzed against distilled water using a cellulose ester dialysis membrane [molecular weight cut off (MWCO) = 3500] for 2 days in order to remove any unreacted reactants.

Conjugation of GA and ciprofloxacin onto CD

GA and ciprofloxacin were conjugated onto CD via EDC chemistry (Scheme: 1). 10 mL amino functionalised CDs (1.5 mg/ mL) were reacted with aqueous solutions of 6.0 mM each of

ciprofloxacin and GA in presence of 20-fold molar EDC at pH ~ 4.2. The reaction mixture is kept at 4°C overnight. The resulting solution containing CD, GA and ciprofloxacin conjugate (CDGAC) was purified by dialysis to remove unreacted CD and GA, as mentioned in the above section and kept refrigerated until use. Unreacted GA obtained after the dialysis of CDGAC was estimated by ninhydrin method[27] and the same was subtracted from the initial amount of GA used in the reaction to get the quantity of GA in the conjugate. The amount of ciprofloxacin conjugated onto CD was calculated from the antibacterial study by Minimum Inhibitory Concentration (MIC) method using tube dilution.

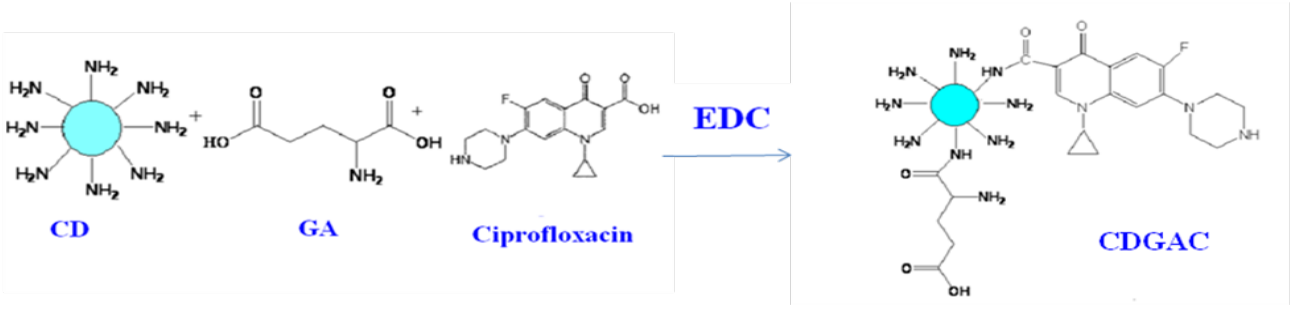

Scheme: 1 Conjugation of GA and ciprofloxacin onto CD

Characterization

High resolution transmission electron microscopy (HRTEM) was performed using an FEI, TECNAI S Twin microscope, Netherland, with an accelerating voltage of 100 kV. The aqueous sample solutions (CD and CDGAC) were prepared by dispersion under an ultrasonic vibrator. They were then deposited on a Formvar-coated copper grid and dried in vacuum at room temperature prior to observation.

Proton Nuclear Magnetic Resonance (H^1NMR) spectra of CD and CDGAC were recorded using 500 MHz Bruker AV 500 NMR spectrometer (Switzerland). Fourier Transform Infra Red (FTIR) spectra of CD and CDGAC were collected in the range 600-4000 cm^{-1} on a Nicolet 5700 FTIR

Spectrometer, Nicolet Inc, Madison, USA using a Diamond ATR accessory. UV-Visible absorption spectra was taken using a UV-Visible spectrophotometer, Varian, Cary 100 Bio, Melbourne, Australia and the fluorescence intensity of the same were measured using a Spectrofluorimeter, Varian, Cary Eclipse model EL 0507, Melbourne, Australia. The technique of Dynamic Light Scattering (DLS), (Malvern Instruments Ltd, UK) was used for the determination of particle size.

Thermogravimetric analysis (TGA) was carried out using Simultaneous DTA–TGA system (SDT Q600, TA Instruments Inc., USA). Approximately 3 mg sample was taken in a platinum cup and heated under nitrogen atmosphere at a heating rate of 10 ºC min^{-1} from room temperature to 900ºC.

Thermal analysis was also carried out with Differential scanning calorimeter (DSC Q100, TA Instruments Inc. USA), using MDSC (Modulated DSC) mode under nitrogen atmosphere at a heating rate of 3 ºC min^{-1} and a modulation amplitude of 1 ºC for a period of 60 s.

The XRD analysis of the materials was carried out using X-ray diffractometer (Bruker, Model-D8 advance, Switzerland).

The in vitro Cytotoxicity study

The *in vitro* cytotoxicity of CDGAC was carried out by direct contact assay as per ISO 10993-5 and by MTT [3-(4,5-dimethylthiazol-2yl)-2,5-diphenyltetrazoliumbriomide] assay as per reported protocol[28].

Direct contact method

CDGAC was filtered through 0.22 µ pore size syringe filter. 40 µL of it was soaked on a filter paper and placed on confluent monolayer of L929 mouse fibroblast cells in triplicate. The negative controls (high density polyethylene) and the positive controls (Stabilised PVC disc) in

triplicate were also placed on cells. After incubation at 37±1 ºC for 24±2 h, cell monolayer was examined microscopically for the response around the test samples. The cytotoxic reactivity of test and control samples was evaluated microscopically (Leica Inverted Fluorecsence Microscope, DMI 6000; Leica microsystem, Wetzlro, Germany).

MTT assay

MTT assay was performed to measure the metabolic activity of cells to reduce yellow coloured tetrazolium salt (MTT) to purple colored formazan. 1 mg of CDGAC was dissolved in 2 mL culture medium containing serum and then diluted to get 25 µg, 12.5 µg and 6.25 µg per 100 µL, and were filtered using 0.22 µ membrane filter. 100 µL of various concentrations of the probe, extract of negative control (Ultra high Molecular Weight Poly Ethylene), cell control and positive control [phenol stock solution diluted (1.3 mg/mL) with culture medium containing serum] were placed on subconfluent monolayer of L-929 cells. After incubation of cells with the samples and controls at 37±1 ºC for 24 ± 2 h, extract and control medium was replaced with 50 µL MTT solution (1mg/ml in medium without supplements), wrapped with aluminium foil and incubated at 37±2 ºC for 2 h. After discarding the MTT solution, 100 µL of isopropanol was added to all wells and swayed the plates. The color developed was quantified by measuring absorbance at 570 nm using a spectrophotometer (Model UVM 340, ASYS, Austria).

Haemolysis assay

Haemolysis assay was carried out as per the report procedure[29]. The collected blood (anticoagulated with sodium citrate) was centrifuged at 1000 rpm for 10 minutes (Sigma, Refrigerated centrifuge, 3-30K, Germany), plasma removed and washed with normal saline and again centrifuged. Supernatant was discarded and the pellet was diluted 1:10 with saline. 100 µL of this was added to 100 µL of the sample (triplicate) and incubated for 45 minutes under

agitation (70±5 rpm) using an orbital shaker (Orbitek, Scigenics, Biotech, Chennai) thermostated at 37±1 ^{o}C. The samples were again centrifuged and supernatant made up to 1 mL with saline and absorbance was measured at 540 nm. Saline was used as the negative control and 1 % Triton-X was used as the positive control. The absorbance for Triton X with maximum haemolysis was taken as 100 % and the extent of haemolysis for the samples were calculated from the respective absorbance.

Determination of antibacterial activity of the conjugate

Antibacterial activity was studied using the bacterial strain *E.coli* (ATCC25922) by Minimum Inhibitory Concentration (MIC) method using tube dilution followed by sub culturing on Muller Hinton Agar. MIC is the lowest concentration that shows clarity in the tube and on subculturing the organism was completely inhibited.

Demonstration of the detection of bone cracks

Freshly collected bone from slaughter house was cleaned and incubated with CDGAC overnight. Thereafter washed, dried and imaged with the Xenogen (Caliper Life Sciences) IVIS Spectrum *in vivo* imaging system (USA) in which quantitative monitoring is possible to visualize the bone cracks selectively targeted by the fluorescent probes.

Results and discussion

CDs passivated with amino terminated PEG were synthesized as reported earlier[26]. The amount of ciprofloxacin and GA on 1 mg CDGAC is quantified as 96 μg and 58 μg respectively. HRTEM micrograph (Fig: 1A) indicates that CDs possess a spherical morphology and have an average size of 4-7 nm which matches with the earlier report[30]. It is clear that the size increased to 55-60 nm as a result of conjugation (Fig: 1B). CDs functionalized with GA and Ciprofloxacin

may interact with one another via H-bonding among the functional groups. Such interaction facilitates the formation of small aggregates. The significant increase in the particle size from 4-7 nm to 55-60 nm on the onset of modification may be assigned to the formation of aggregrated structures. Similar observations have been reported earlier[25, 31]. To support this observation, DLS measurements on CD and CDGAC were carried out. The average size for CD and CDGAC were found to be 10 $\pm$ 3.0 nm and 137 $\pm$ 7.0 nm respectively (Table S1, supporting information) which are higher than the values obtained from TEM analysis. It is already reported from our group that DLS measurement records higher values for particle size since the light is scattered by the core as well as the layers formed on the surface of the particles[32]. Further, from TEM analysis the number-average particle size is obtained whereas DLS gives the z-average particle size[33]. Similar observations have been reported earlier also[34].

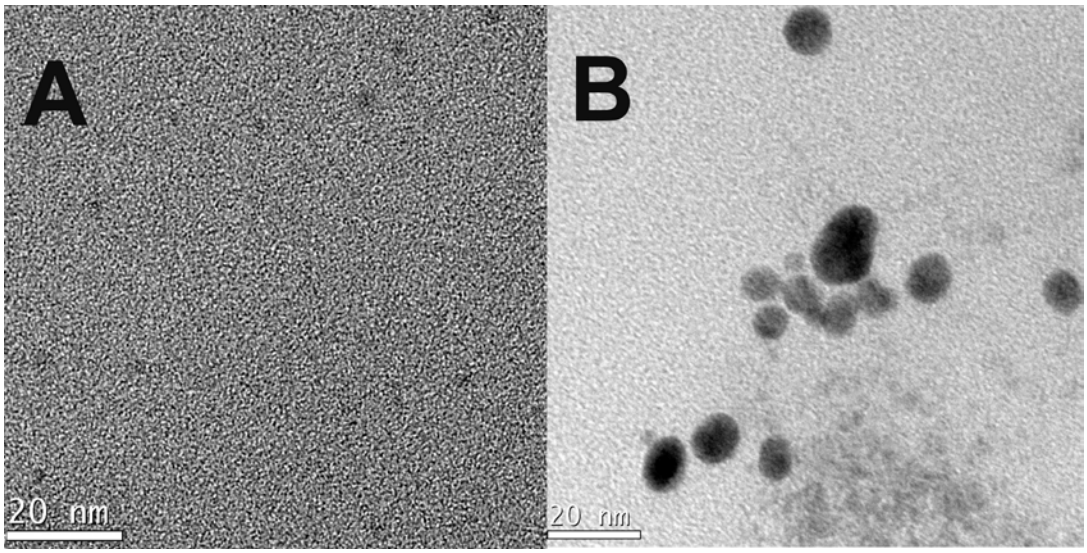

Fig: 1 HRTEM micrograph of A) CD and B) CDGAC

FTIR spectra (Fig: S1, supporting information) reflect the conjugation of GA and ciprofloxacin onto CDs. Bands associated with amide bonds can be seen at 1638 cm^{-1} (-CO- stretching) and 1560 cm^{-1} (-N-H bending) for CDGAC. Characterstic peak of CDs seen at 2870 cm^{-1} is shifted to

2970 cm^{-1} due to conjugation. Further indication of the modification can be seen from the ^{1}H NMR spectra of CD and CDGAC (Figs. S2A and S2B in the supporting information). The peak at δ= 3.6 ppm is attributed to the methylene group of PEG diamine (used for the synthesis of CD) which could be detected in the ^{1}H NMR spectra of both CD and CDGAC. The additional peaks at 3.3, 1.0 and 2.8 ppm in CDGAC confirm the conjugation of ciprofloxacin and GA onto CD. The signals observed at 3.3 ppm and 1.0 ppm were assigned to the aliphatic hydrogen atoms in ciprofloxacin[35]. The peak at 2.8 ppm corresponds to the methylene group of GA.

To get additional information on the modified CDs, thermogravimetric analysis was carried out. TGA of CD and CDGAC are shown in Fig: S3 (supporting information). CDGAC is decomposed at a faster rate when compared to CD. Around 650ºC the residual weight of CD is 9.5 % whereas for CDGAC it is 6.9 %. The conjugation may probably be affecting the interaction between CDs since the functional groups are being used for the coupling of drug molecules and glutamic acid. XRD pattern of CD (Fig: S4, supporting information) shows a strong peak at 2θ=19.24º with interlayer spacing (d value) 4.6 Aº and a weak peak is also observed at 2θ=23.14º with d value 3.8 Aº. Pan et al have shown that carbon nanoparticles possess a graphitic nature with interlayer spacing 4.2 Aº, larger than that of bulk graphite (3.3 Aº) [36]. The sharp peak around 19.24º is assigned to PEG chains by conducting XRD analysis of PEG diamine (PEGD) used for the synthesis of CDs (Fig: S4). This was confirmed by MDSC scan. MDSC trace showed a melting peak around 29 ºC (Fig: S5) which was assigned to the melting of PEGD associated with CDs by running a separate MDSC analysis on PEGD (Fig: S5) [though pure PEGD melted at higher temperature (51 ºC)]. CDs after modification with drug and GA also showed more or less similar thermal behavior.

UV-Visible absorption spectra of CD and CDGAC are depicted in Fig: S6 in the supporting information. In addition to the characteristic absorption peak of CD around 360 nm, CDGAC showed peak at 272 nm associated with ciprofloxacin, further confirming its presence in the conjugate.

The fluorescence emission spectra of CD and CDGAC are shown in Fig: S7 in the supporting information. The photographic images of aqueous CD (A) and CDGAC (B) in day light (A&B) and under UV light (A_1 & B_1) are shown in the inset. It can be seen that conjugation of GA and ciprofloxacin do not have any observable effect on the fluorescing characteristics of the CD under UV light.

Both CD and CDGAC show emission peak maximum around 450 nm when excited at a wavelength of 360 nm again showing that modification is not affecting the inherent fluorescence of CD.

Emission spectra of CDGAC at various excitations are given in Fig: 2. As the excitation wavelength of CDGAC increases, the peak emission shifts slightly to longer wavelengths causing a reduction in the fluorescence intensity. The maximum emission intensity is observed at an excitation wavelength of 360 nm and this wavelength is fixed for further studies. It is a known fact that CDs exhibit different emissions depending on excitation wavelengths[30] and such varied optical features are said to be due to the size distribution of CD or emission trap distribution on CD surfaces[37].

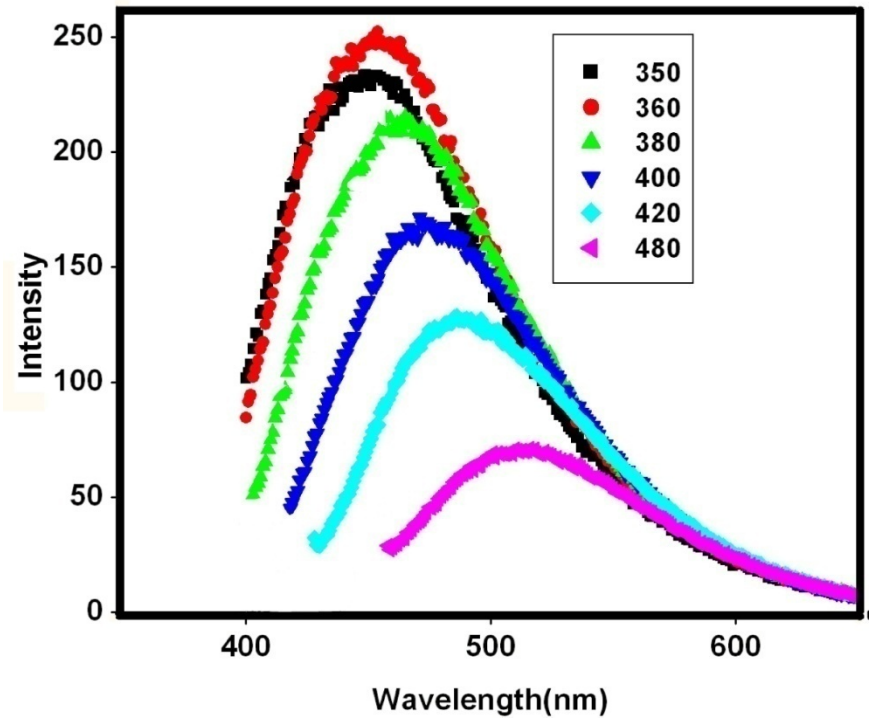

Fig: 2 Emission spectra of CDGAC at various excitations

Fig: 3A proves that direct deposition of CDGAC onto a confluent layer of L929 fibroblast cells has no reactivity to them after 24 h of contact. As per ISO 10993-5 the achievement of numerical grade more than 2 is considered as cytotoxic effect. Since the test material, CDGAC achieved a numerical grade zero, the material is considered to be non-cytotoxic. The material does not cause any lysis, degeneration or loss of spindle shape morphology of the cells further confirming their non cytotoxicity. Fig: 3B and 3C are the images for positive control and negative control respectively on contact with L929 cells.

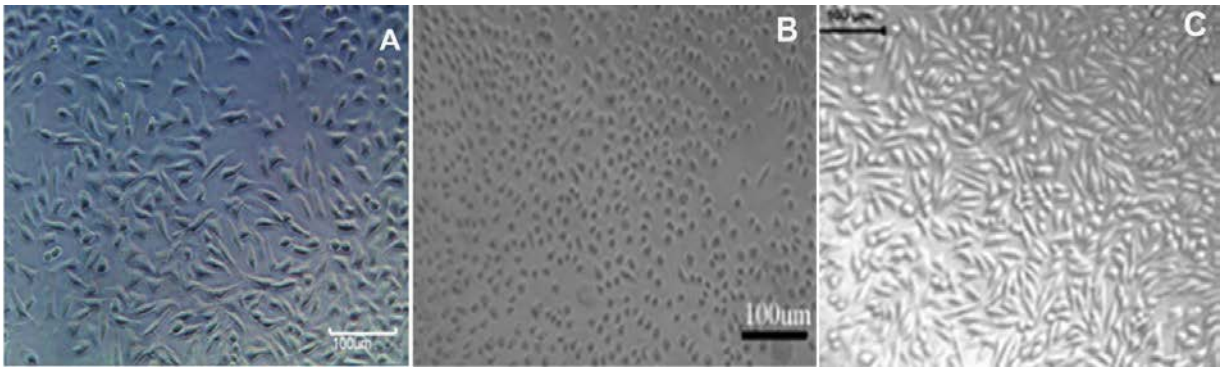

Fig: 3 *In vitro* cytotoxicity study- Direct contact method

A) CDGAC B) PVC (positive control) and C) HDPE (negative control)

Quantitative assessment of the cytotoxicity of cells on contact with 25 µg, 12.5 µg and 6.25 µg of CDGAC showed 108 %, 120 % and 109 % metabolic activity respectively (Fig: 4). The results are the average of three replicate experiments. According to the statistical analysis, Percentage viability of the samples is significantly high when compared to the positive control (phenol). These results affirm that modified CDs are noncytotoxic.

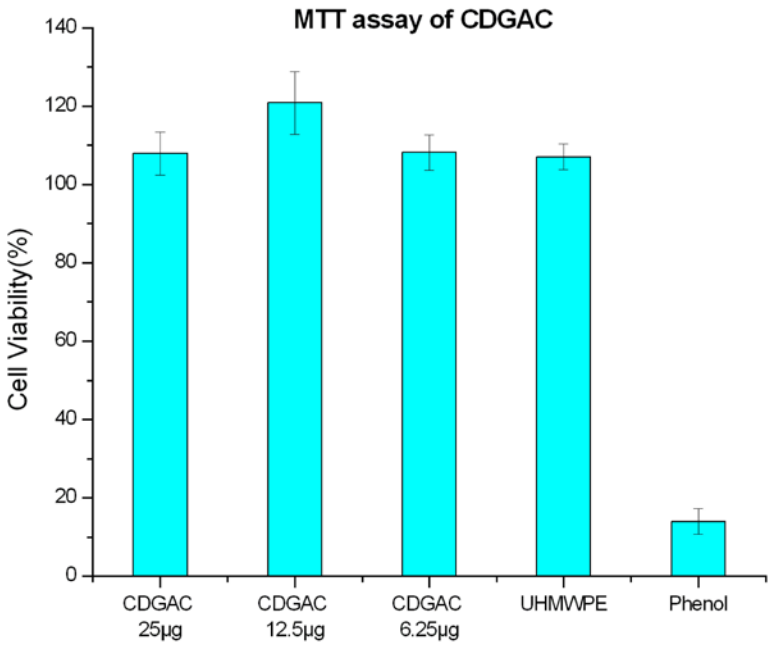

Fig: 4 Cytotoxicity assessed by MTT assay.

Percentage haemolysis for different concentrations of CD and CDGAC are shown in Fig: S8 in the supporting information. Samples 1 to 5 correspond to CD 1 mg/mL, CD 0.5 mg/mL, CD 0.25 mg/mL, CDGAC 1 mg/mL and CDGAC 0.5 mg/mL respectively. Photographic images are shown in the inset of Fig: S8. According to the ASTM E2524-08, if the assay result for a test-nanomaterial falls below 2 %, the material is considered non-haemolytic; haemolysis values between 2 and 5 % are interpreted as moderately haemolytic and those above 5 % qualify the test-nanomaterial as haemolytic[38,39]. It is clear from the figure that our samples are non–haemolytic with values < 1 %.

Microbial inhibition assay of CDGAC was carried out. Ciprofloxacin(C), CD and CDGAC were taken in the same Petri dish (using double dilutions in Petri dishes with serial numbers 1, 2,3,4,5 and 6 respectively) as shown in Fig: 5. It can be seen that CDs showed scanty bacterial growth for the first two cases, moderate growth in the third and heavy growth for the remaining concentrations. The scanty growth may be due to the nonspecific inhibition by the comparatively high concentration of CD. However, the bacterial growth (bacterial strain *E.coli*) is inhibited by the probe (CDGAC) at varying concentrations, starting from 0.5 mg/mL (Table S2 in the supporting information), upto 1:32 dilutions (Petri dish no.6 in Fig 5). The study revealed that the MIC of the standard ciprofloxacin for the bacteria ATCC 25922 E coli determined using tube dilution method is 1.5 μg/mL and the amount of ciprofloxacin conjugated on 1 mg CDGAC is quantified as 96 μg. The results further prove that CDGAC itself is antibacterial and for checking bacterial infection, the drug need not be cleaved from the probe.

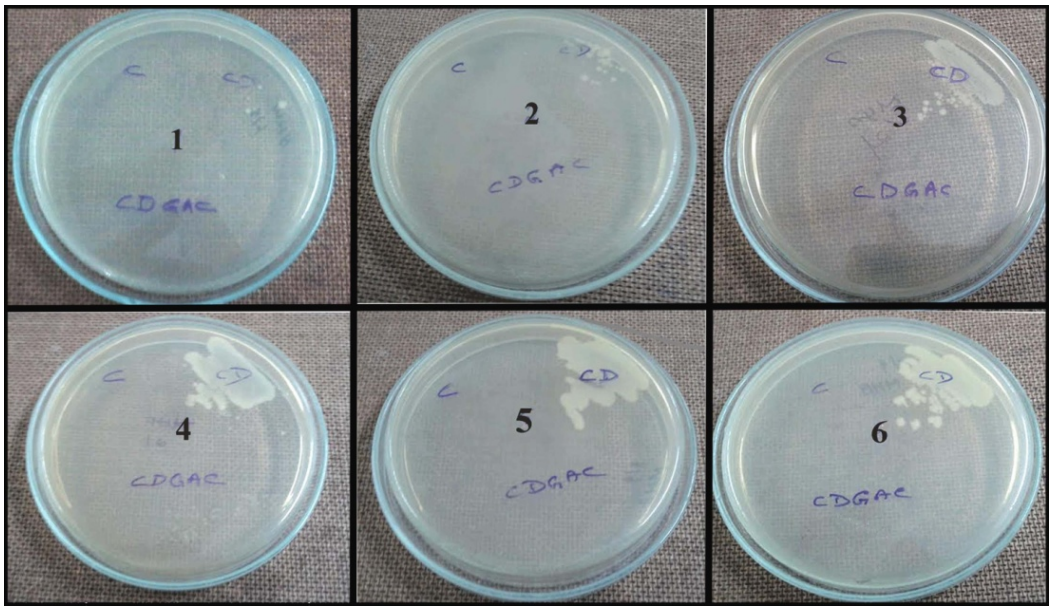

Fig: 5 Antibacterial study with CD, CDGAC and C (Ciprofloxacin, Sigma). Sl. Nos 1-6 show doubling dilutions starting from 0.5 mg/mL for CD & CDGAC and 50 mg/mL for C

The conjugated ciprofloxacin was found to be active even after one month under refrigerated condition reflecting that the shelf life of the probe is appreciable.

We assessed the stability of the drug conjugate at pH 7.4. Purified CDGAC was kept in a dialysis bag membrane, MWCO = 3500 and immersed in PBS (pH 7.4) for 24 h and measured the UV absorbance of the PBS (Fig S9 B in the supporting information) to know the release of ciprofloxacin from the conjugate due to hydrolysis. It is clear that trace B didn't show any significant absorption for ciprofloxacin indicating that CDGAC is stable at pH 7.4. This observation substantiates that the probe can dock onto the target without any leakage of the drug in physiological fluids like blood (pH 7.4).

The studies done so far confirm that the probe synthesized here is highly fluorescent in nature and possesses excellent antibacterial property. Additionally, GA on the probe could guide it towards calcium rich sites like bone crack. We attempted to demonstrate this feature of the probe with freshly collected bones from slaughter house. The bones were cleaned, a crack made on the

surface manually and incubated with CDGAC for 24 h. Thereafter washed, dried and imaged with the Xenogen (Caliper Life Sciences) IVIS Spectrum in vivo imaging system to locate the bound CDGAC on the crack of the bone surface. The image was taken at an excitation wavelength of 430 nm since the machine doesn't have shorter excitation wavelength. It is evident from Fig: 2 that the CDGAC can also be excited at this wave length, though the maximum emission is obtained at 360 nm. The color bar indicates that the red region is the area of maximum fluorescence intensity. From the image given in Fig: 6 it is evident that the bone crack region (marked) is red in colour confirming the maximum binding of the probe at the cracked site. This result apparently suggests the ability of the probe to concentrate and thereby to locate even minor bone cracks.

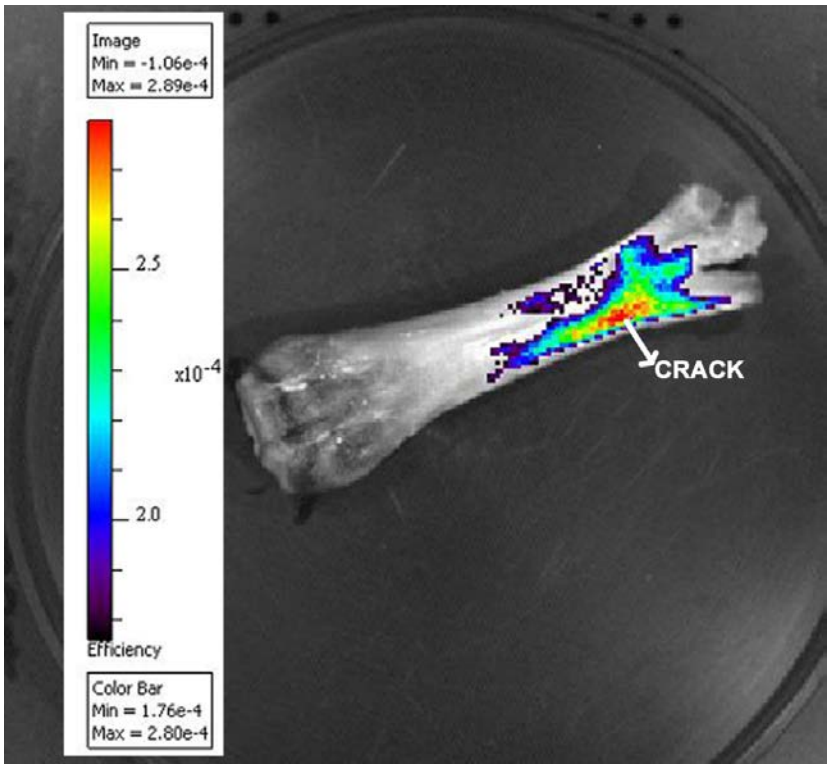

Fig: 6 Bone crack detection (marked) by CDGAC imaged with IVIS system.

Conclusions

Bone targeting nanoparticle drug delivery system based on fluorescent CDs was successfully synthesized. The system was found to be non cytotoxic, hemocompatible and antibacterial in nature, and was also proved to be useful for bone crack detection as well as drug deposition at the cracked sites to control infection. Interestingly, as in many drug delivery approaches, in this case there is no need for the cleavage of the drug from the conjugate to show activity since the modified probe itself is antibacterial.

Acknowledgement

Authors wish to thank DBT and ICMR New Delhi for financial support. Authors are also grateful to Mr. Vijayan, for XRD, Tissue culture laboratory, SCTIMST for Cytotoxicity studies, Biophotonics laboratory, SCTIMST for IVIS Spectrum invivo imaging system and NIIST, Trivandrum for Proton NMR and HRTEM facilities.

References

1. M. Bruchez, M. Moronne, P. Gin, S. Weiss, and A.P. Alivisatos, *Science,* 1998, **281**, 2013–2015.
2. W. C. W. Chan, and S. M. Nie, *Science,* 1998, **281**, 2016–2018.
3. L. Loomba, and T. Scarabelli, *Ther Deliv,* 2013, **4**, 1179-96.
4. T. Asefa, C.T. Duncanc, and K.K. Sharma, *Analyst*, 2009**, 134**, 1980–1990.
5. L. Zhou, Z. Li, Z. Liu, J. Ren, and X. Qu, *Langmuir*, 2013, **29**, 6396–6403.
6. S. Karthik, B. Saha, K. S. Ghosh, and N. D. P. Singh, *Chem. Commun,* 2013, **49**, 10471—10473.
7. W. Shi, X. Li, and H. Ma, *Angew. Chem. Int. Ed,* 2012, **124**, 6538 –6541.
8. S. N. Baker, and G. A. Baker, *Angew. Chem. Int. Ed,* 2010, **49**, 2−21.

9. F. Wang, Z. Xie, H. Zhang, C. Liu, and Y. Zhang, *Adv. Funct. Mater*, 2011, **21**, 1027−1031.
10. A. Zhu, Q. Qu, X. Shao, B. Kong, and Y. Tian, *Angew. Chem. Int. Ed*, 2012, **51**, 7185 –7189.
11. H. Tao, K. Yang, Z. Ma, J. Wan, Y. Zhang, Z. Kang, and Z. Liu, *Small*, 2012, **8**, 281−290.
12. S. Qu, H. Chen, X. Zheng, J. Cao, and X. Liu, *Nanoscale*, 2013, **5**, 5514–5518.
13. W. Gu, C. Wu, J. Chen, and Y. Xiao, *Int J Nanomedicine*, 2013, **8,** 2305-17.
14. C. S. Colon-Emeric, *J. Am. Med. Assoc*, 2006, **296**, 2968–2969.
15. D. G. Anderson, J. A. Burdick, and R. Langer, *Science*, 2004, **305**, 1923-4.
16. M. E. Gindy, and R. K . Prud'homme, *Expert Opin Drug Deliv*, 2009, **6,** 865-78.
17. T. Luhmann, O. Germershaus, J. Groll, and L. Meinel, *J. Controlled Release*, 2012, **161**, 198 – 213
18. V. Yadav, J. D. Freedman, M. Grinstaff, and A. Sen, *Angew Chem Int Ed*, 2013, **52**, 10997–11001.
19. W. Marshall, J. *Clinical Chemistry, Mosby, London, 3rd edn*, 1995, ISBN 0-7234-2190-0.
20. R. D. Ross, and R. K. Roeder, *J Nanopart Res*, 2012, **14**, 1175.
21. K. Yokogawa, K. Miya, T. Sekido, Y. Higashi, M. Nomura, R. Fujisawa, K. Morito, Y. Masamune, Y. Waki, S. Kasugai, and K. Miyamoto, *Endocrinology*, 2001, **142**, 1228-1233.
22. J. M. Nelson, T. M. Chiller, J. H. Powers, and F. J. Angulo, *Clin Infect Dis*, 2007, **44**, 977–980.
23. P. R. Odgren, and T. J. Martin, *Science*, 2000, **289**, 1508-1514.

24. D. Wang, S. Miller, M. Sima, P. Kopeckova, and J. Kopecek, *Bioconjugate Chem*, 2003, **14**, 853-859.

25. A. Shanti Krishna, C. Radhakumary, and K. Sreenivasan, *Analyst*, 2013, **138**, 7107–7111.

26. F. Wang, S. Pang, L. Wang, Q. Li, M. Kreiter, and C. Liu, *Chem. Mater*, 2010, **22**, 4528 – 4530.

27. H. Meyer, *Biochem. J*, 1957, **67**, 333-340

28. G. Ciapetti, E. Cenni, L. Pratelli, and A. Pizzoferato, *Biomaterials*, 1993, **14**, 359-64.

29. M. R. Rekha, and C.P. Sharma, *Biomaterials*, 2009, **30**, 6655-6664

30. E. Goh, K. S. Kim, Y. R. Kim, H. S. Jung, S. Beack, W. S. Kong, G. Scarcelli, S. H. Yun, and S. K. Hahn, *Biomacromolecules*, 2012, **13**, 2554−2561.

31. Z. Ye, R. Tang, H. Wu, B. Wang, M. Tan, and J. Yuana, *New J. Chem*, 2014, DOI: 10.1039/c4nj00966e

32. C. Radhakumary, and K. Sreenivasan, *Anal. Chem*, 2011, **83**, 2829–2833

33. M. Babic, D. Horak, P. Jendalova, K. Glogarova, V. Herynek, M. Trchova, K. Likavanova, P. Lesny, E. Pollert, M. Hajek, and E. Sykova, *Bioconjugate Chem*. 2009, **20**, 283–294

34. Y. Q. He, S. P. Liu, L. Kong, and Z. F. Liu, *Spectrochim.Acta*, *PartA*. 2005, **61**, 2861–2866

35. A. Zieba, A. Maslankiewicz, and Sitkowski, J. *Magn. Reson. Chem*, 2004, **42**, 903–904.

36. D. Y. Pan, J .C. Zhang, W. Q. Shen, Z. W. Zhang, Y. G. Fang, and M. H. Wu, *New J. Chem*, 2010, **34**, 591–593.

37. H. Zhu, X. Wang, Y. Li, Z. Wang, F. Yang, and X. Yang, Chem. Commun, 2009**, 34**, 5118−5120.

38. Standard Test Method for Analysis of Hemolytic Properties of Nanoparticles, Active standard, ASTM E2524-08 (2013), ASTM International.

39. M. A. Dobrovolskaia, and S. E. McNeil, *J Control Release*, 2013, **172**, 456-66

Graphical Abstract

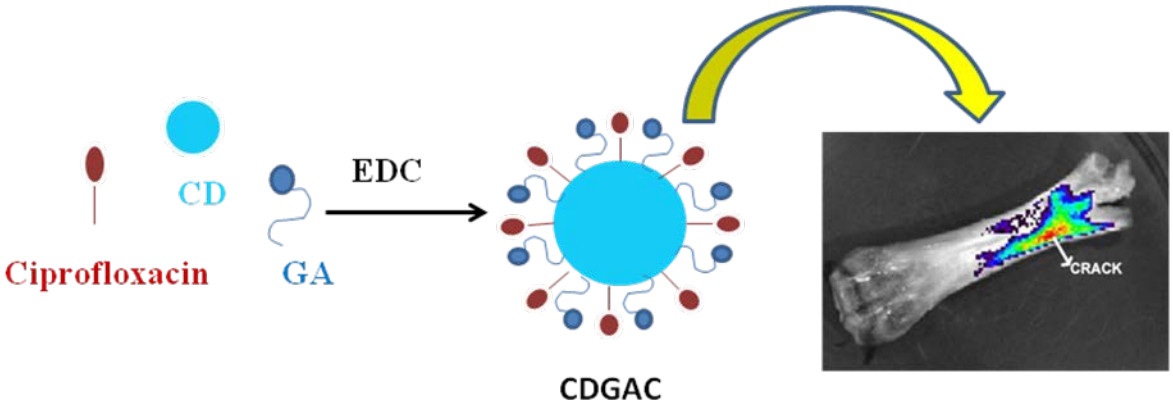

Decorated carbon dots enable simultaneous bone crack viewing and drug deposition.